Synchronization under saturable nonlinearity

Journal Article

Author(s):
Stoychev, Alexander K.; Pedergnana, Tiemo; Noiray, Nicolas

Publication date:
2024-08

Permanent link:
https://doi.org/https://doi.org/10.3929/ethz-b-000688255

Originally published in:
Chaos 34(8), https://doi.org/10.1063/5.0222816

Synchronization under saturable nonlinearity

Cite as: Chaos 34, 081102 (2024); doi: 10.1063/5.0222816
Submitted: 10 June 2024 · Accepted: 12 July 2024 ·
Published Online: 1 August 2024

Alexander K. Stoychev,[a] Tiemo Pedergnana, and Nicolas Noiray[a]

AFFILIATIONS

CAPS Laboratory, Department of Mechanical and Process Engineering, ETH Zürich, 8092 Zürich, Switzerland

[a]**Authors to whom correspondence should be addressed:** astoychev@ethz.ch and noirayn@ethz.ch

ABSTRACT

In this theoretical work, we introduce a nonlinear gain saturation law representative of the experimentally observed properties manifested by phenomena ranging from aeroacoustic shear layers in self-sustained cavity oscillations to flame heat release rate in thermoacoustic instabilities. Furthermore, this type of saturable gain may be relevant for a wider class of physical systems, such as active laser media in photonics. The nonlinearity discussed herein governs the fullscale behavior of a self-oscillator exhibiting linear loss under large amplitude perturbations, in contrast to the cubic damping and linear gain of the Van der Pol model. A distinctive characteristic of the proposed equation is the simple, well behaved gain term in the slow timescale dynamics.

Synchronization phenomena are ubiquitous in nature and have been a source of fruitful developments in numerous branches of engineering and physics. Nevertheless, most studies thereon consider systems close to a (supercritical) Hopf bifurcation, where the amplitude dynamics is governed by the Stuart–Landau equation. The prototypical model featuring such behavior is the Van der Pol oscillator. However, the corresponding cubic nonlinearity generally fails to reproduce the physical response away from the bifurcation point where the limit cycle amplitudes may be significant.

I. INTRODUCTION

Synchronization is an emergence phenomenon observed in weakly interacting dynamical and complex systems exhibiting a self-sustained recurrent state evolution.[1] Particular instances thereof range from neuroscience[2] and human cognition,[3] through biological[4] and neural networks,[5] to abstract dynamical systems[6,7] and populations of oscillators.[8] In this study, we focus on the (deterministic) forced synchronization between (immutable) external excitation and a single limit cycle oscillator.[1,6]

The ability of a nonautonomous outside forcing to alter the (self-sustained) natural dynamics of a system, i.e., forced synchronization, provides an important prospect for interaction with weakly coupled (to the environment) scattering elements, such as cavity modes. However, developments utilizing the prototypical limit cycle oscillator described by the VdP equation have to be physically compatible with the quadratically diverging resistance term.[9] Nevertheless, researchers from various fields such as acoustics,[10–12] optics,[13,14] and electromagnetics,[15–17] have recognized that the dissipative cubic nonlinearity and linear gain of the VdP model are often inappropriate and saturable gain combined with linear dissipation is better suited for many applications.

For example, a nominally stable shear layer is able to amplify acoustic perturbations at certain frequencies. The proximity of an acoustic mode eigenfrequency to this amplifying range is a condition for the emergence of self-sustained cavity oscillations in flow-grazed resonators[10,11,18] and some musical instruments, such as the flute. However, as observed experimentally[10] and theoretically,[18] this behavior eventually saturates due to nonlinear effects and the systems flips from finite linear gain at low amplitudes to finite linear loss at high ones. Therefore, to model the acoustic impedance of a grazed aperture,[10,18] we need to utilize a saturable nonlinearity law compatible with this phenomenon.

One possibility is to introduce a gain saturation directly into the averaged (slow timescale) equations without considering the primitive (fullscale) formulation,[11] or to analyze the latter only via numerical methods. However, this makes validation of the averaged equations, and by extension any analytical work thereon, difficult. Therefore, further research into nonlinear gain saturation laws is necessary, on both the fullscale and averaged dynamics level.

In the following, we introduce and thoroughly investigate the fullscale nonlinear dynamical system yielding an (averaged) amplitude equation governed by the saturation model[13,14,16] $g(a) = (1 + a^2)^{-1}$. Subsequently, we explore the synchronization properties of the amplitude equations and compare them to the fullscale dynamics.

II. OSCILLATOR MODEL

In contrast to many other physical modeling tasks, the study of synchronization is usually based on simple, phenomenological, reduced order models of the form[1]

$$\ddot{x} + f(x, \dot{x}) + x = F \cos \Omega\tau. \tag{1}$$

The differential operator $\dot{(\cdot)} = \mathrm{d}/\mathrm{d}\tau$ denotes the (dimensionless) time derivative, while F and Ω are the (dimensionless) amplitude and (normalized) frequency of the excitation, respectively. The main object of interest in this section is the nonconservative term $f(x, \dot{x})$, which governs the nonlinear dynamics of the system and determines its synchronization properties.

A. Fullscale dynamics

Consider a nonconservative term of the form

$$f(x, \dot{x}) = \mu(1 + \psi(x))\dot{x}, \tag{2}$$

where μ denotes the bifurcation parameter, which can also be interpreted as a constant resistance term, and $\psi(x)$ is the nonlinearity. In particular, we introduce a nonlinear gain saturation model ($\lim_{x\to\infty} \psi(x) = 0$) compatible with the behavior of various physical systems[10,12,13]

$$\psi(x) = \frac{3x \sinh^{-1} x}{(1 + x^2)^{5/2}} - \frac{2 - x^2}{(1 + x^2)^2} \tag{3}$$

and which, to the best of our knowledge, has not been considered elsewhere. Additional discussion of its mathematical properties can be found in Appendix A.

For the specific $f(x, \dot{x})$ given in (2), the autonomous part of Eq. (1) reduces to the second order oscillator

$$\ddot{x} + \mu\left(1 + \frac{3x \sinh^{-1} x}{(1 + x^2)^{5/2}} - \frac{2 - x^2}{(1 + x^2)^2}\right)\dot{x} + x = 0. \tag{4}$$

Therefore, the following statement holds.

Corollary 1. *For any $\mu > 0$, the planar system (4) has a unique, stable, and globally attractive limit cycle.*

Proof. First we identify that Eq. (4) has the form $\ddot{x} + \mu d(x)\dot{x} + k(x) = 0$, with $d(x) = 1 + \psi(x)$ and $k(x) = x$, hence, we can apply the Liénard theorem (p. 254 in Ref. 19). In particular, the Liénard transform $y = -D(x) - \dot{x}/\mu$, with

$$D(x) = \int_0^x (1 + \psi(x))\mathrm{d}x = -\frac{\sinh^{-1} x}{(1 + x^2)^{3/2}} + \frac{x^3}{1 + x^2}, \tag{5}$$

yields the following first order system:

$$\dot{x} = \mu\left(\frac{\sinh^{-1} x}{(1 + x^2)^{3/2}} - \frac{x^3}{1 + x^2} - y\right), \tag{6}$$

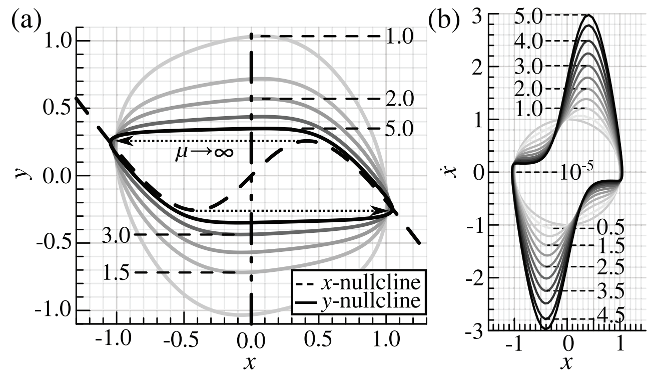

FIG. 1. Phase space representation of the global attractor for different values of the bifurcation parameter $\mu > 0$ in (a) Liénard transformed $x - y$ and (b) $x - \dot{x}$ coordinate system.

$$\dot{y} = \frac{1}{\mu}x. \tag{7}$$

To verify the conditions of the Liénard theorem, consider

1. Both $D'(x) = d(x) = 1 + \psi(x)$ and $k'(x) = 1$ have no singularities for $x \in \mathbb{R}$, hence, the smoothness requirements of $D(x), k(x) \in C^1(\mathbb{R})$ are satisfied. In fact, both are in $C^\infty(\mathbb{R})$.
2. Both $k(x) = x = -(-x) = -k(-x)$ and
$$D(x) = -\frac{\sinh^{-1} x}{(1 + x^2)^{3/2}} + \frac{x^3}{1 + x^2} = \frac{\sinh^{-1}(-x)}{(1 + (-x)^2)^{3/2}} - \frac{(-x)^3}{1 + (-x)^2} = -D(-x)$$
are odd functions.
3. $k(x) = x > 0 \ \forall x > 0$.
4. $D(x)$ has roots only for $x \in \{-\tilde{x}, 0, \tilde{x}\}$ and the slope $D'(x) = d(x) > 0 \ \forall x > \tilde{x}$, where $\tilde{x} \approx 0.84$. This can be corroborated by inspection of the Liénard system (6) and (7) and, in particular, its x-nullcline, i.e., $y = -D(x)$, which is depicted in Fig. 1(a).
5. $D'(0) = d(0) = -1 < 0$
6. $\lim_{x\to\infty} D(x) = x \to \infty$,

which implies the system has exactly one limit cycle and it is stable. Furthermore, analyzing the (static) x- and y-nullclines, illustrated in Fig. 1(a) and given by

$$y = \frac{\sinh^{-1} x}{(1 + x^2)^{3/2}} - \frac{x^3}{1 + x^2}, \tag{8}$$

$$x = 0, \tag{9}$$

respectively, we can determine that they intersect only at the origin. Hence, this is the only fixed point of the system and it is unstable, since the sum of the eigenvalues is $\mathrm{tr}([\mu \ \ -\mu; 1/\mu \ \ 0]) = \mu > 0$. Additionally, there are no solutions diverging to infinity; therefore, the limit cycle will attract all trajectories away from the origin. □

Inspection of Fig. 1(a) reveals that at large values of the bifurcation parameter, i.e., $\mu \gg 0$, the system behaves as relaxation oscillator, analogous to the Van der Pol model. Furthermore, from Fig. 1(b) we can deduce that for $\mu \ll 1$ the behavior of (4) is similar to a Stuart–Landau equation. Therefore, in the latter case, an asymptotic averaging[20] can be expected to accurately capture the dominant dynamical features of the system.

B. Slow timescale dynamics

In this section, we focus on the weak nonlinearity limit, derive the amplitude equations via averaging,[20] and examine their properties. Following the standard treatment of weakly nonlinear self-oscillators,[1,6] we consider slow deviations from the (linear) conservative solution

$$x(\tau) = A(\tau)\cos\left(\Omega\tau + \varphi(\tau)\right), \tag{10}$$

$$\dot{x}(\tau) = -\Omega A(\tau)\sin\left(\Omega\tau + \varphi(\tau)\right), \tag{11}$$

where the oscillation amplitude $A(\tau)$ and phase $\varphi(\tau)$ are defined via Eqs. (10) and (11) as

$$A(\tau) = \sqrt{x^2(\tau) + \left(\frac{\dot{x}(\tau)}{\Omega}\right)^2}, \tag{12}$$

$$\varphi(\tau) = -\tan^{-1}\left(\frac{\dot{x}(\tau)}{\Omega x(\tau)}\right) - \Omega\tau. \tag{13}$$

Taking the time derivative of Eqs. (12) and (13), while recalling (1), results in

$$\dot{A} = \frac{\Omega^2 - 1}{\Omega^2 A}x\dot{x} - \frac{\dot{x}}{\Omega^2 A}\left(f(x,\dot{x}) - F\cos\Omega\tau\right), \tag{14}$$

$$\dot{\varphi} = \frac{1-\Omega^2}{\Omega A^2}x^2 + \frac{x}{\Omega A^2}\left(f(x,\dot{x}) - F\cos\Omega\tau\right), \tag{15}$$

where all arguments have been dropped for convenience.

Subsequently, under the assumption of weak nonlinearity, we integrate over one forcing period, invoking Bogoliubov's theorem[20] of slow timescale evolution, obtaining

$$\dot{A} = -\langle f(x,\dot{x})|\dot{x}\rangle - \frac{F\sin\varphi}{2\Omega}, \tag{16}$$

$$\dot{\varphi} = \Delta + \frac{1}{\Omega A}\langle f(x,\dot{x})|x\rangle - \frac{F\cos\varphi}{2\Omega A}, \tag{17}$$

with $\Delta = (1-\Omega^2)/2\Omega$ and an inner product $\langle\cdot|\cdot\rangle$ reading

$$\langle f(x,\dot{x})|\dot{x}\rangle = \frac{1}{2\pi\Omega A}\int_0^{\frac{2\pi}{\Omega}} f(x(\tau),\dot{x}(\tau))\dot{x}(\tau)\mathrm{d}\tau. \tag{18}$$

Since the integrals involving $f(x,\dot{x})$ are not trivial to evaluate, henceforth we consider the problem in power series form. The closed Maclaurin expansion of $\psi(x)$ reads

$$\psi(x) = \sum_{n=0}^{\infty}\psi_n x^{2n} = \sum_{n=0}^{\infty}\frac{(-2)^{n+1}(n+1)!}{(2n-1)!!}x^{2n}, \tag{19}$$

where $(\cdot)!$ and $(\cdot)!!$ denote the standard and double factorial, respectively. Utilizing Eq. (19) and $\phi = \Omega\tau + \varphi$ implies the inner products in (16) and (17) evaluate to

$$\langle f|\dot{x}\rangle = \mu\frac{A}{2} + \mu\Omega^2 A^2\sum_{n=0}^{\infty}\psi_n\langle\cos^{2n}\phi|\sin^2\phi\rangle A^{2n}, \tag{20}$$

$$\langle f|x\rangle = -\mu\Omega A^2\sum_{n=0}^{\infty}\psi_n\langle\cos^{2n}\phi|\sin\phi\cos\phi\rangle A^{2n}. \tag{21}$$

The inner products between powers of sine and cosine in Eqs. (20) and (21) can be expressed analytically as

$$\langle\cos^{2n}\phi|\sin^2\phi\rangle = \frac{1}{\Omega^2 A}\frac{(2n-1)!!}{2^{n+1}(n+1)!} = \frac{1}{\Omega^2 A}\frac{1}{|\psi_n|}, \tag{22}$$

$$\langle\cos^{2n}\phi|\sin\phi\cos\phi\rangle = 0, \tag{23}$$

ultimately resulting in

$$\langle f|\dot{x}\rangle = \mu\frac{A}{2} - \mu\sum_{n=0}^{\infty}(-1)^n A^{2n+1} = \mu\frac{A}{2} - \frac{\mu A}{1+A^2}, \tag{24}$$

$$\langle f|x\rangle = 0. \tag{25}$$

Substituting Eqs. (24) and (25) into (16) and (17), respectively, yields the slow timescale dynamics

$$\dot{A} = \frac{\mu}{2}\left(\frac{1-A^2}{1+A^2}\right)A - \frac{F\sin\varphi}{2\Omega}, \tag{26}$$

$$\dot{\varphi} = \Delta - \frac{F\cos\varphi}{2\Omega A}. \tag{27}$$

The equivalent complex form,[11] i.e., $a = Ae^{j\varphi}$, reads

$$\dot{a} = \left(j\Delta + \frac{\mu}{2}\frac{1-|a|^2}{1+|a|^2}\right)a - j\frac{F}{2\Omega}, \tag{28}$$

where j and $|\cdot|$ denote the imaginary unit and the modulus, respectively. As a consequence of the averaging,[20] limit cycles in the fullscale system (1) correspond to fixed points in the averaged equations (26) and (27). This greatly simplifies the bifurcation analysis presented below.

III. BIFURCATION ANALYSIS

Next, we derive analytic expressions for the bifurcation curves defining the 1:1 Arnold (synchronization) tongue and discuss their implications for the fullscale system.

Since we are searching for fixed points of Eqs. (26) and (27), cf. Fig. 3, we can set $\dot{A} = 0$ and $\dot{\varphi} = 0$

$$\frac{1 - A_0^2}{1 + A_0^2} A_0 = \frac{F}{\mu\Omega} \sin\varphi_0, \tag{29}$$

$$\underbrace{\frac{2\Delta}{\mu}}_{\delta} A_0 = \underbrace{\frac{F}{\mu\Omega}}_{\mathcal{F}} \cos\varphi_0, \tag{30}$$

where the φ dependence can be eliminated by squaring and summing Eqs. (29) and (30), resulting in

$$\left(1 - A_0^2\right)^2 A_0^2 + \delta^2 (1 + A_0^2)^2 A_0^2 = (1 + A_0^2)^2 \mathcal{F}^2. \tag{31}$$

Equation (31) is a bicubic polynomial and, therefore, its roots appear in pairs symmetric with respect to zero. Since $A \in \mathbb{R}^+$ by definition, we can introduce the coordinate transform $A_0 = \sqrt{B}$ and bring (31) to the form

$$aB^3 + bB^2 + cB + d = 0, \tag{32}$$

with coefficients defined as

$$a = 1 + \delta^2, \tag{33}$$

$$b = -2 + 2\delta^2 - \mathcal{F}^2, \tag{34}$$

$$c = 1 + \delta^2 - 2\mathcal{F}^2, \tag{35}$$

$$d = -\mathcal{F}^2, \tag{36}$$

and a discriminant reading

$$D = b^2c^2 - 4ac^3 - 4b^3d + 18abcd - 27a^2d^2. \tag{37}$$

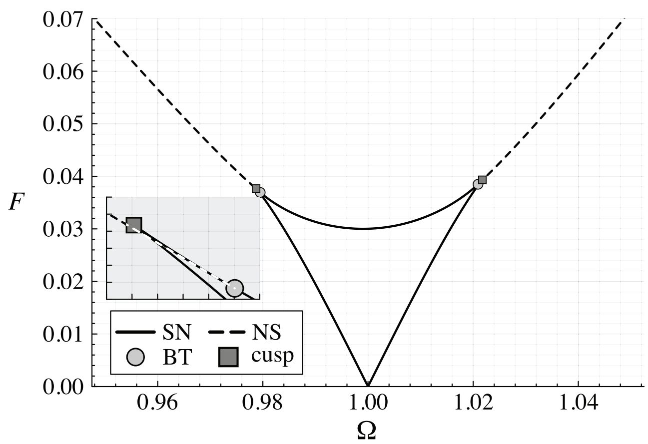

FIG. 2. Bifurcation map of the two dimensional parameter space $F - \Omega$ ($\mu = 0.1$). Solid lines indicate the continuous branches of saddle-node bifurcations in (26) and (27) and fold of cycles in (1), respectively. Dashed lines depict branches of Andronov–Hopf bifurcations in (26) and (27) and Neimark–Sacker in (1). Circular markers represent Bogdanov–Takens bifurcations in (26) and (27) and strong 1:1 resonance in (1). Square markers indicate cusp bifurcations. The inset shows a detailed view around the codimension two bifurcation points.

A. Bifurcations of codimension one

From $a > 0$ and $d < 0$, we can deduce that Eq. (32) has either one ($D < 0$) or three ($D > 0$) positive real roots, corresponding to one and three fixed points of (26) and (27) or limit cycles of (1), cf. Fig. 3. At $D = 0$, a saddle and an (un)stable fixed point in (26) and (27) merge and disappear via a saddle-node bifurcation, which corresponds to a fold of limit cycles[7] in the primitive (fullscale) system (1).

Substituting (33)–(36) into (37), constraining $D = 0$, and performing some algebraic manipulations yield an expression for the 1D manifolds of saddle-node (fold of cycles) bifurcations separating the $D > 0$ synchronization region [cf. Figs. 2, 3, and 4(a)]

$$\mathcal{F}^2_{1,2} = -\delta^2 - \frac{11}{3} + \frac{4}{3}\sqrt{31 + 3^3\delta^2} \times \cos\left(\frac{1}{3}\cos^{-1}\left(\frac{\frac{2^6}{3^3} - \left(\frac{67}{27} + \delta^2\right)^2}{\frac{2^4}{3^6}(31 + 27\delta^2)^{\frac{3}{2}}}\right) - \frac{(1 \pm 1)\pi}{3}\right). \tag{38}$$

The relation between the non-normalized bifurcation parameters F and Ω can be trivially obtained by substituting $\mathcal{F} = F/\mu\Omega$ and $\delta = (1 - \Omega^2)/\mu\Omega$ into (38). Since $\mu, F, \Omega \in \mathbb{R}^+$ by definition, the negative roots for $\mathcal{F}$ can be omitted. Additionally, the saddle-node (fold of cycles) bifurcation is only possible for $\delta^2 \leq 5/27$ and $\mathcal{F}^2 \leq 4/27$ (cf. Figs. 2 and 3), while $D < 0$ and $\mathcal{F}_{1,2} \in \mathbb{C}$ otherwise.

The amplitude at the critical equilibrium (limit cycle), where the saddle-node (fold of cycles) bifurcation occurs, is calculated by substituting (33)–(36) into (32) and evaluating the double root from its depressed form (Fig. 3)

$$A_0^2 = \frac{1 - \mathcal{F}^4 - \delta^4 - 2\mathcal{F}^2(3 + \delta^2)}{1 + \mathcal{F}^4 - 14\delta^2 + \delta^4 + 2\mathcal{F}^2(5 + \delta^2)}. \tag{39}$$

Of course, at the special points $\delta = \pm\sqrt{5/27}$ all roots merge and (39) is undefined. The amplitude then reads

$$A_0^2 = \frac{2(1 - \delta^2) + \mathcal{F}^2}{3(1 + \delta^2)}. \tag{40}$$

We proceed with evaluating the stability (cf. Fig. 3) of the fixed points by analyzing the Jacobian of (26) and (27)

$$J(\mathcal{F}, \delta) = \frac{\mu}{2}\begin{bmatrix} \frac{1 - A^2}{1 + A^2} - \left(\frac{2A}{1 + A^2}\right)^2 & -\mathcal{F}\cos\varphi \\ \frac{\mathcal{F}}{A^2}\cos\varphi & \frac{\mathcal{F}}{A}\sin\varphi \end{bmatrix}. \tag{41}$$

Since we are interested in the (eigen)spectrum of the Jacobian evaluated at an equilibrium, we can make use of the relationships (29) and (30) to remove the φ dependence. Substituting $\mathcal{F}/A_0 \sin\varphi_0 = (1 - A_0^2)/(1 + A_0^2)$ and $\mathcal{F}/A_0 \cos\varphi_0 = \delta$ into (41) then yields

$$J(\mathcal{F}, \delta) = \frac{\mu}{2}\begin{bmatrix} \frac{1 - A_0^2}{1 + A_0^2} - \left(\frac{2A_0}{1 + A_0^2}\right)^2 & -\delta A_0 \\ \frac{\delta}{A_0} & \frac{1 - A_0^2}{1 + A_0^2} \end{bmatrix}. \tag{42}$$

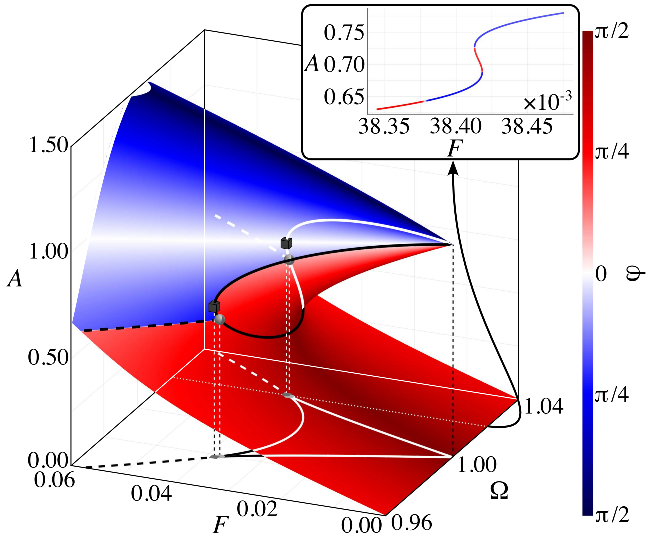

FIG. 3. Synchronization (steady state) amplitude, A, phase, φ, and stability as a function of the two dimensional parameter space $F - \Omega$ ($\mu = 0.1$). The phase is depicted by the color map, where blue (red) shades indicate stability (instability). Solid lines indicate the continuous branches of saddle-node (fold of cycles) bifurcations and their projection onto the $F - \Omega$ plane corresponds to the lower region in Fig. 2. Dashed lines depict branches of Andronov–Hopf (Neimark–Sacker) bifurcations and their projection coincides with the upper region in Fig. 2. Cube markers with square projection represent cusp bifurcations. Sphere markers with circular projection indicate Bogdanov–Takens (strong 1:1 resonance) bifurcations. The inset shows an $A - F$ plane section at $\Omega = 1.0215$ capturing the bistable region between codimension two bifurcation points.

The problem's low dimensional nature permits derivation of the stability criterion from $\mathrm{tr}(J) < 0 \wedge \det(J) > 0$. Fixed points with $A_0 \geq 1$ are unconditionally stable (cf. Fig. 3) and for the case of $A_0 < 1$ we have

$$\left(\frac{1-A_0^2}{1+A_0^2}\right)^2 < \frac{1-A_0^2}{1+A_0^2}\left(\frac{A_0^4+4A_0^2-1}{(1+A_0^2)^2}\right) < \delta^2. \tag{43}$$

Outside the $D > 0$ synchronization region [cf. Fig. 4(a)] bounded by (38) (cf. Figs. 2 and 3), the system (26) and (27) has only one fixed

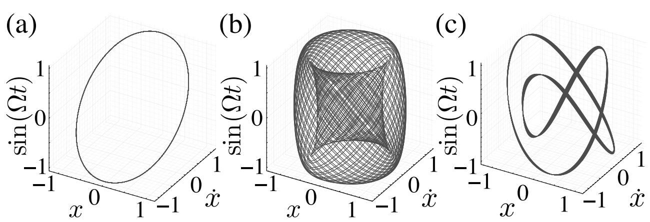

FIG. 4. Representative trajectories of the fullscale system (1) depicting the long time dynamics (a) inside the 1:1 Arnold (synchronization) tongue, (b) in its vicinity, and (c) far away from it (cf. Fig. 2). In particular, the individual sub-panels show (a) a synchronized limit cycle, (b) an invariant torus emerging from the Neimark–Sacker bifurcation manifold, and (c) an attractor with non-trivial topology.

point, which naturally raises the questions of how and when it looses stability. In particular, if we study the marginally stable states, from the first condition in (43) we can deduce that

$$A_0^2 = \sqrt{2} - 1 \tag{44}$$

always holds. The second condition in (43) then implies

$$\delta^2 \geq (\sqrt{2} - 1)^2. \tag{45}$$

The marginal stability defined by (44) and (45) corresponds to an Andronov–Hopf bifurcation in (26) and (27) and Neimark–Sacker (torus birth) bifurcation of cycles[7] in (1) [cf. Fig. 4(b)]. Naturally, an equilibrium in (26) and (27) with amplitude defined as (44) implies relation between the (normalized) bifurcation parameters $\mathcal{F}, \delta$. To determine $\mathcal{F}(\delta)$, we substitute (44) into (31), resulting in

$$\mathcal{F}^2 = \left(\sqrt{2} - 1\right)\left(\delta^2 + \left(\sqrt{2} - 1\right)^2\right). \tag{46}$$

Once more, an expression in the non-normalized bifurcation parameters F and Ω can be simply obtained by substituting $\mathcal{F} = F/\mu\Omega$ and $\delta = (1 - \Omega^2)/\mu\Omega$ into (46), where the result is depicted as a dashed line in Figs. 2 and 3.

B. Bifurcations of codimension two

In the slow timescale dynamics (26) and (27), we have two saddle-node and two Andronov–Hopf branches, making all three generic codimension two bifurcations of time continuous planar systems[7] possible. In particular, any saddle-node branch could contain a cusp bifurcation, the Andronov–Hopf branches could support a Bautin bifurcation, and a Bogdanov–Takens can be located on either.

Starting from the latter, we note that the origins of the two Andronov–Hopf branches (46) defined by $\delta \geq \sqrt{2} - 1$ and $\delta \leq 1 - \sqrt{2}$ satisfy $\mathrm{tr}(J) = 0$ and $\det(J) = 0$. Therefore, at those points, J exhibits a zero eigenvalue with double multiplicity, i.e., the signature of a Bogdanov–Takens (BT) bifurcation. Consequently, a couple of BT points can be found at $\delta = \pm(\sqrt{2} - 1)$ and $\mathcal{F} = \sqrt{2}(\sqrt{2} - 1)^{3/2}$ (cf. $\bullet$ in Figs. 2 and 3). Of course, the aforementioned points must also belong to a saddle-node branch, due to the zero eigenvalues. In this case, the two Andronov–Hopf merge with the "-" branch in (38) (cf. Figs. 2 and 3). In the primitive (fullscale) system (1), this corresponds to a Neimark–Sacker (torus birth) bifurcation of cycles branch merging with fold of cycles one via a strong resonance,[7] in this case 1:1.

Now we turn our attention to the cusp bifurcations, which are characterized by a simple eigenvalue of J equal zero (implying location on a saddle-node branch) and vanishing quadratic coefficient in the (one dimensional) normal form[7] of the bifurcation. Investigation of (26) and (27) yields an analytically tractable existence condition

$$\frac{4A(A_0^2 - 3)}{(1 + A_0^2)^3} + \frac{(1 + A_0^2)^3\delta^4}{(1 - A_0^2)^3 A_0} + \frac{(1 + A_0^2)\delta^2}{(1 - A_0^2)A_0} = 0. \tag{47}$$

For $\delta = \pm\sqrt{5/27}$, $\mathcal{F} = \sqrt{4/27}$ and the resulting amplitude from (40), condition (47) is satisfied, thus verifying the occurrence of two cusp bifurcation where saddle-node branches merge (cf. ■ in Figs. 2 and 3). Furthermore, it can be shown that none of the other points on the branches (38) and their corresponding amplitudes (39) satisfy (47), thus ruling out any additional cusp bifurcations. In the primitive (fullscale) system (1), the cusp corresponds to three limit cycles merging together and disappearing.[7]

Finally, the first Lyapunov coefficient along the Andronov–Hopf branches can be shown to be strictly negative, i.e., $l_1 < 0$. Therefore, we conclude they are supercritical and no Bautin bifurcations ($l_1 = 0$) occur thereon, at least not in the 1:1 synchronization region.

IV. CONCLUSION

In this study, we introduce a novel synchronization model and thoroughly investigate its natural dynamics and forced synchronization properties.

The equation proposed in Sec. II shows some convenient similarities to the Van der Pol system, such as (1) relaxation oscillations at large values of the bifurcation parameter and (2) Stuart–Landau type of behavior at small ones. However, the model discussed above exhibits saturable gain at large amplitudes in contrast to the quadratically diverging term in the VdP oscillator, which renders it more appropriate for the modeling of many physical systems. In particular, the oscillation amplitudes in the weakly nonlinear regime are governed by the common saturation law $g(a) = (1 + a^2)^{-1}$, which has been successfully utilized in the modeling of a wide variety of physical phenomena.

Subsequently, Sec. III presents the derivation of analytical expressions for the continuum of codimension one bifurcations defining the 1:1 Arnold (synchronization) tongue. In particular, the equilibria of the slow timescale (averaged) equations and their implications for the fullscale dynamics are studied. For the considered subset of 2D parameter space (and fixed $\mu = 0.1$), the theoretical results are indistinguishable from a numerical bifurcation analysis of the primitive fullscale system.

Nevertheless, the theory, naturally, has some limitations and should not be taken out of context. Despite capturing all of the relevant dynamical properties of the weakly nonlinear, weakly forced system, the averaging procedure does alter the dynamics and some of its features are lost. In particular, the forced fullscale system can and does exhibit the presence of Chenciner (generalized Neimark–Sacker) bifurcations and the corresponding complex dynamics.[7] Furthermore, at certain parameter values, the primitive formulation exhibits attractors of non-trivial topology [cf. Fig. 4(c)], which cannot be represented by the (planar) averaged dynamics.

One important influence that falls beyond the scope of this study is the effect of additive and multiplicative noise. In particular, the averaging procedure in such case is slightly altered,[20] resulting in an additional term, inversely proportional to the amplitude, and noise in both variables. The investigation of the system behavior then proceeds by analyzing the steady state statistics of the associated Fokker–Plank equation, which needs to be derived for the saturable nonlinearity discussed above.

AUTHOR DECLARATIONS

Conflict of Interest

The authors have no conflicts to disclose.

Author Contributions

Alexander K. Stoychev: Conceptualization (equal); Formal analysis (lead); Investigation (lead); Methodology (lead); Validation (lead); Visualization (lead); Writing – original draft (lead). **Tiemo Pedergnana:** Conceptualization (equal); Methodology (supporting); Supervision (supporting); Writing – original draft (supporting). **Nicolas Noiray:** Conceptualization (equal); Funding acquisition (lead); Methodology (supporting); Project administration (lead); Supervision (lead); Writing – original draft (supporting).

DATA AVAILABILITY

Data sharing is not applicable to this article as no new data were created or analyzed in this study.

APPENDIX A: SATURABLE NONLINEARITY LAW

The distinctive properties of the saturable gain nonlinearity (3) are illustrated in Fig. 5. Sub-panel (a) shows the unit ($\mu = 1$) resistance term of the fullscale oscillator (1) and (b) depicts the loss term in the averaged dynamics (26) and (27). The gain and loss terms are plotted separately and the VdP model is shown as a reference.

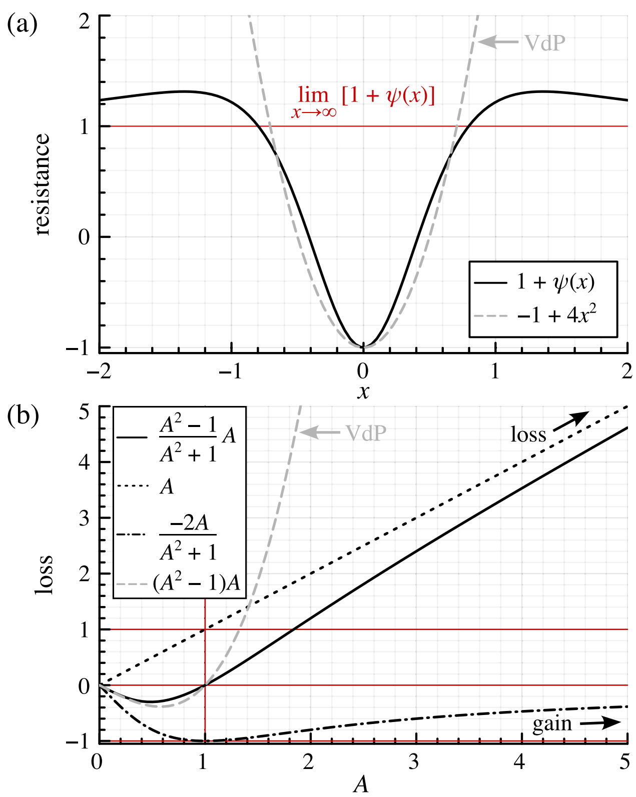

FIG. 5. Behavior of the proposed nonlinearity and the VdP model in terms of (a) resistance in the fullscale formulation and (b) gain/loss in the slow timescale (averaged) dynamics.

REFERENCES

[1]A. Pikovsky, M. Rosenblum, and J. Kurths, *Synchronization: A Universal Concept in Nonlinear Science*, Cambridge Nonlinear Science Series No. 12 (Cambridge University Press, 2001).
[2]W. Singer, "Neuronal synchrony: A versatile code for the definition of relations?,"Neuron **24**, 49–65 (1999).
[3]W. Condon and W. Ogston, "Sound film analysis of normal and pathological behavior patterns," J. Nerv. Mental Dis. **143**, 338–347 (1966).
[4]S. Strogatz and I. Stewart, "Coupled oscillators and biological synchronization," Sci. Am. **269**, 102–109 (1993).
[5]J. Collins, C. Chow, and T. Imhoff, "Stochastic resonance without tuning," Nature **376**, 236–238 (1995).
[6]A. Balanov, N. Janson, D. Postnov, and O. Sosnovtseva, *Synchronization: From Simple to Complex* (Springer, 2008).
[7]Y. A. Kuznetsov, *Elements of Applied Bifurcation Theory*, Applied Mathematical Sciences Vol. 112 (Springer, 2013).
[8]S. Strogatz, "From kuramoto to crawford: Exploring the onset of synchronization in populations of coupled oscillators," Physica D **143**, 1–20 (2000).
[9]N. Noiray and B. Schuermans, "Deterministic quantities characterizing noise driven hopf bifurcations in gas turbine combustors," Int. J. Non-Linear Mech. **50**, 152–163 (2013).
[10]C. Bourquard, A. Faure-Beaulieu, and N. Noiray, "Whistling of deep cavities subject to turbulent grazing flow: Intermittently unstable aeroacoustic feedback," J. Fluid Mech. **909**, A19 (2021).
[11]T. Pedergnana and N. Noiray, "Superradiant scattering by a limit cycle," Phys. Rev. Appl. **20**, 034068 (2023).
[12]N. Noiray, "Linear growth rate estimation from dynamics and statistics of acoustic signal envelope in turbulent combustors," J. Eng. Gas Turb. Power **139**, 041503 (2017).
[13]A. E. Siegman, *Lasers* (University Science Books, 1986).
[14]H. Wang, S. Assawaworrarit, and S. Fan, "Dynamics for encircling an exceptional point in a nonlinear non-hermitian system," Opt. Lett. **44**, 638–641 (2019).
[15]S. Assawaworrarit, X. Yu, and S. Fan, "Robust wireless power transfer using a nonlinear parity–time-symmetric circuit," Nature **546**, 387–390 (2017).
[16]K. Bai, J. Li, T. Liu, L. Fang, D. Wan, and M. Xiao, "Nonlinear exceptional points with a complete basis in dynamics," Phys. Rev. Lett. **130**, 266901 (2023).
[17]K. Bai, T. Liu, L. Fang, J. Li, C. Lin, D. Wan, and M. Xiao, "Observation of nonlinear exceptional points with a complete basis in dynamics," Phys. Rev. Lett. **132**, 073802 (2024).
[18]A. Stoychev, T. Pedergnana, and N. Noiray, "Nonlinear acoustics of an aperture under grazing flow," Proc. R. Soc. A **480**, 20230718 (2024).
[19]L. Perko, *Differential Equations and Dynamical Systems* (Springer, 2013), Vol. 7.
[20]N. M. Krylov and N. N. Bogoliubov, *Introduction to Non-linear Mechanics* (Princeton University Press, 1950), Vol. 11.